First Measurement of the CP-Violating Phase in $B_s^0 \to \phi\phi$ Decays

R. Aaij *et al.**
(LHCb Collaboration)

(Received 28 March 2013; published 12 June 2013)

A first flavor-tagged measurement of the time-dependent CP-violating asymmetry in $B_s^0 \to \phi\phi$ decays is presented. In this decay channel, the CP-violating weak phase arises due to CP violation in the interference between B_s^0-$\bar{B}_s^0$ mixing and the $b \to s\bar{s}s$ gluonic penguin decay amplitude. Using a sample of pp collision data corresponding to an integrated luminosity of 1.0 fb^{-1} and collected at a center-of-mass energy of 7 TeV with the LHCb detector, 880 $B_s^0 \to \phi\phi$ signal decays are obtained. The CP-violating phase is measured to be in the interval $[-2.46, -0.76]$ rad at a 68% confidence level. The p value of the standard model prediction is 16%.

DOI: 10.1103/PhysRevLett.110.241802 PACS numbers: 13.25.Hw, 11.30.Er, 12.15.Hh, 14.40.Nd

The $B_s^0 \to \phi\phi$ decay is forbidden at the tree level in the standard model (SM) and proceeds via a gluonic $b \to s\bar{s}s$ penguin process. Hence, this channel provides an excellent probe of new heavy particles entering the penguin quantum loops [1–3]. Generally, CP violation in the SM is governed by a single phase in the Cabibbo-Kobayashi-Maskawa quark mixing matrix [4]. The interference between the B_s^0-$\bar{B}_s^0$ oscillation and decay amplitudes leads to a CP asymmetry in the decay time distributions of B_s^0 and $\bar{B}_s^0$ mesons, which is characterized by a CP-violating weak phase. The SM predicts this phase to be small. Due to different decay amplitudes the actual value is dependent on the B_s^0 decay channel. For $B_s^0 \to J/\psi\phi$, which proceeds via a $b \to c\bar{c}s$ transition, the SM prediction of the weak phase is given by $-2\arg(-V_{ts}V_{tb}^*/V_{cs}V_{cb}^*) = -0.036 \pm 0.002$ rad [5]. The LHCb Collaboration recently measured the weak phase in this decay to be $0.068 \pm 0.091\,(\text{stat}) \pm 0.011\,(\text{syst})$ rad [6], which is consistent with the SM and places stringent constraints on CP violation in B_s^0-$\bar{B}_s^0$ oscillations [7]. In the SM, the phase in the $B_s^0 \to \phi\phi$ decay ϕ_s is expected to be close to zero due to a cancellation of the phases arising from B_s^0-$\bar{B}_s^0$ oscillations and decay [8]. Calculations using QCD factorization provide an upper limit of 0.02 rad for $|\phi_s|$ [1–3].

In this Letter, we present the first measurement of the CP-violating phase in $B_s^0 \to \phi\phi$ decays. Charge conjugate states are implied. The result is based on pp collision data corresponding to an integrated luminosity of 1.0 fb^{-1} and collected by the LHCb experiment in 2011 at a center-of-mass energy of 7 TeV. This data sample was previously used for a time-integrated measurement of the polarization amplitudes and triple product asymmetries in the same decay mode [9]. The analysis reported here improves the selection efficiency, measures the B_s^0 decay time, and identifies the flavor of the B_s^0 meson at production. This allows a study of CP violation in the interference between mixing and decay to be performed. It is necessary to disentangle the CP-even longitudinal (A_0), CP-even transverse ($A_\parallel$), and CP-odd transverse ($A_\perp$) polarizations of the $\phi\phi$ final state by measuring the distributions of the helicity angles [9].

The LHCb detector is a forward spectrometer at the Large Hadron Collider covering the pseudorapidity range $2 < \eta < 5$ and is described in detail in Ref. [10]. Events are selected by a hardware trigger, which selects hadron or muon candidates with high transverse energy or momentum (p_T), followed by a two stage software trigger [11]. In the software trigger, $B_s^0 \to \phi\phi$ candidates are selected either by identifying events containing a pair of oppositely charged kaons with an invariant mass close to that of the ϕ meson or by using a topological b-hadron trigger. In the simulation, pp collisions are generated using PYTHIA 6.4 [12], with a specific LHCb configuration [13]. Decays of hadronic particles are described by EVTGEN [14] and the detector response is implemented using the GEANT4 toolkit [15] as described in Ref. [16].

The $B_s^0 \to \phi\phi$ decays are reconstructed by combining two ϕ meson candidates that decay into the K^+K^- final state. Kaon candidates are required to have $p_T > 0.5$ GeV/c, and an impact parameter χ^2 larger than 16 with respect to the primary vertex (PV), where the impact parameter χ^2 is defined as the difference between the χ^2 of the PV reconstructed with and without the considered track. Candidates must also be identified as kaons using the ring-imaging Cherenkov detectors [17], by requiring that the difference in the global likelihood between the kaon and pion mass hypotheses ($\Delta\ln\mathcal{L}_{K\pi} \equiv \ln\mathcal{L}_K - \ln\mathcal{L}_\pi$) be larger than -5. Both ϕ meson candidates must have a reconstructed mass m_{KK} of the kaon pair within 20 MeV/c^2 of the known mass of the ϕ meson, a transverse momentum (p_T^ϕ) larger than

*Full author list given at the end of the article.

0.9 GeV/c, and a product $p_{\mathrm{T}}^{\phi 1} p_{\mathrm{T}}^{\phi 2} > 2$ GeV$^2/c^2$. The χ^2 per degree of freedom (ndf) of the vertex fit for both ϕ meson candidates and the B_s^0 candidate is required to be smaller than 25. Using the above criteria, 17 575 candidates are selected in the invariant four-kaon mass range $5100 < m_{KKKK} < 5600$ MeV/c^2.

A boosted decision tree (BDT) [18] is used to separate signal from background. The six observables used as input to the BDT are p_{T}, η, and χ^2/ndf of the vertex fit for the B_s^0 candidate and the cosine of the angle between the B_s^0 momentum and the direction of flight from the closest primary vertex to the decay vertex, in addition to the smallest p_{T} and the largest track χ^2/ndf of the kaon tracks. The BDT is trained using simulated $B_s^0 \to \phi\phi$ signal events and background from the data where at least one of the ϕ candidates has invariant mass in the range $20 < |m_{KK} - m_\phi| < 25$ MeV/c^2.

The *sPlot* technique [19,20] is used to assign a signal weight to each $B_s^0 \to \phi\phi$ candidate. Using the four-kaon mass as the discriminating variable, the distributions of the signal components for the B_s^0 decay time and helicity angles can be determined in the data sample. The sensitivity to ϕ_s is optimized taking into account the signal purity and the flavor tagging performance. The final selection of $B_s^0 \to \phi\phi$ candidates based on this optimization is required to have a BDT output larger than 0.1, $\Delta \ln \mathcal{L}_{\mathrm{K}\pi} > -3$ for each kaon, and $|m_{KK} - m_\phi| < 15$ MeV/c^2 for each ϕ candidate.

In total, 1182 $B_s^0 \to \phi\phi$ candidates are selected. Figure 1 shows the four-kaon invariant mass distribution for the selected events. Using an unbinned extended maximum likelihood fit, a signal yield of 880 ± 31 events is obtained. In this fit, the $B_s^0 \to \phi\phi$ signal component is modeled by two Gaussian functions with a common mean. The width of the first Gaussian component is measured to be 12.9 ± 0.5 MeV/c^2, in agreement with the expectation from simulation. The relative fraction and width of the second Gaussian component are fixed from simulation to values of 0.785 and 29.5 MeV/c^2, respectively, in order to ensure a good quality fit. Combinatorial background is modeled using an exponential function which is allowed to vary in the fit. Contributions from specific backgrounds such as $B^0 \to \phi K^{*0}$, where $K^{*0} \to K^+\pi^-$, are found to be negligible.

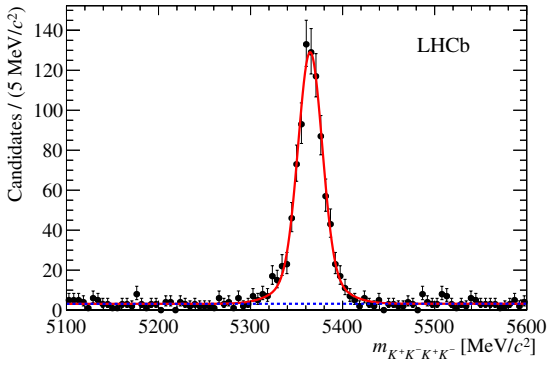

FIG. 1 (color online). Invariant $K^+K^-K^+K^-$ mass distribution for selected $B_s^0 \to \phi\phi$ candidates. The total fit (solid line) consists of a double Gaussian signal component together with an exponential background (dotted line).

An unbinned maximum likelihood fit is performed to the decay time t and the three helicity angles $\Omega = \{\theta_1, \theta_2, \Phi\}$ of the selected $B_s^0 \to \phi\phi$ candidates, each of which is reassigned a signal *sPlot* weight based on the four-kaon invariant mass m_{KKKK} [19,20]. The probability density function (PDF) consists of signal components, which include detector resolution and acceptance effects, and are factorized into separate terms for the decay time and the angular observables.

The B_s^0 decay into the $K^+K^-K^+K^-$ final state can proceed via combinations of intermediate vector (ϕ) and scalar ($f_0(980)$) resonances and scalar nonresonant K^+K^- pairs. Thus the total decay amplitude is a coherent sum of P-wave (vector-vector), S-wave (vector-scalar) and SS-wave (scalar-scalar) contributions. The differential decay rate of the decay time and helicity angles is described by a sum of 15 terms, corresponding to five polarization amplitudes and their interference terms

$$\frac{d^4\Gamma}{d\cos\theta_1 d\cos\theta_2 d\Phi dt} \propto \sum_{i=1}^{15} K_i(t) f_i(\Omega). \qquad (1)$$

The angular functions $f_i(\Omega)$ for the P-wave terms are derived in Ref. [21] and the helicity angles of the two ϕ mesons are randomly assigned to θ_1 and θ_2. The time-dependent functions $K_i(t)$ can be written as [21]

$$K_i(t) = N_i e^{-\Gamma_s t}\Big[c_i \cos(\Delta m_s t) + d_i \sin(\Delta m_s t) + a_i \cosh\Big(\frac{1}{2}\Delta\Gamma_s t\Big) + b_i \sinh\Big(\frac{1}{2}\Delta\Gamma_s t\Big)\Big], \qquad (2)$$

where $\Delta\Gamma_s = \Gamma_{\mathrm{L}} - \Gamma_{\mathrm{H}}$ is the decay width difference between the light (L) and heavy (H) B_s^0 mass eigenstates, Γ_s is the average decay width, $\Gamma_s = (\Gamma_{\mathrm{L}} + \Gamma_{\mathrm{H}})/2$, and Δm_s is the B_s^0-$\bar{B}_s^0$ oscillation frequency. The coefficients N_i, a_i, b_i, c_i, and d_i can be expressed in terms of ϕ_s and the magnitudes $|A_i|$ and phases δ_i of the five polarization amplitudes at $t = 0$. The three P-wave amplitudes, denoted by A_0, $A_\parallel$, $A_\perp$, are normalized such that $|A_0|^2 + |A_\parallel|^2 + |A_\perp|^2 = 1$, with the strong phases δ_1 and δ_2 defined as $\delta_1 = \delta_\perp - \delta_\parallel$ and $\delta_2 = \delta_\perp - \delta_0$. The S- and SS-wave amplitudes and their corresponding phases are denoted by A_S, A_{SS}, and δ_S, δ_{SS}, respectively. For a B_s^0 meson produced at $t = 0$, the coefficients in Eq. (2) and the angular functions $f_i(\theta_1, \theta_2, \Phi)$ are given in Table I, where $\delta_{2,1} = \delta_2 - \delta_1$. Assuming that CP violation in mixing and direct CP violation are negligible, the differential distribution for a $\bar{B}_s^0$ meson is obtained by changing the sign of the coefficients c_i and d_i. The PDF is invariant under the transformation $(\phi_s, \Delta\Gamma_s, \delta_\parallel, \delta_\perp, \delta_S, \delta_{SS}) \to (\pi - \phi_s,$

TABLE I. Coefficients of the time-dependent terms and angular functions defined in Eqs. (1) and (2). Amplitudes are defined at $t = 0$.

i	N_i	a_i	b_i	c_i	d_i	f_i
1	$\lvert A_0\rvert^2$	1	$-\cos\phi_s$	0	$\sin\phi_s$	$4\cos^2\theta_1\cos^2\theta_2$
2	$\lvert A_\parallel\rvert^2$	1	$-\cos\phi_s$	0	$\sin\phi_s$	$\sin^2\theta_1\sin^2\theta_2(1+\cos2\Phi)$
3	$\lvert A_\perp\rvert^2$	1	$\cos\phi_s$	0	$-\sin\phi_s$	$\sin^2\theta_1\sin^2\theta_2(1-\cos2\Phi)$
4	$\lvert A_\parallel\rvert\lvert A_\perp\rvert$	0	$-\cos\delta_1\sin\phi_s$	$\sin\delta_1$	$-\cos\delta_1\cos\phi_s$	$-2\sin^2\theta_1\sin^2\theta_2\sin2\Phi$
5	$\lvert A_\parallel\rvert\lvert A_0\rvert$	$\cos(\delta_{2,1})$	$-\cos(\delta_{2,1})\cos\phi_s$	0	$\cos(\delta_{2,1})\sin\phi_s$	$\sqrt{2}\sin2\theta_1\sin2\theta_2\cos\Phi$
6	$\lvert A_0\rvert\lvert A_\perp\rvert$	0	$-\cos\delta_2\sin\phi_s$	$\sin\delta_2$	$-\cos\delta_2\cos\phi_s$	$-\sqrt{2}\sin2\theta_1\sin2\theta_2\sin\Phi$
7	$\lvert A_{SS}\rvert^2$	1	$-\cos\phi_s$	0	$\sin\phi_s$	4/9
8	$\lvert A_S\rvert^2$	1	$\cos\phi_s$	0	$-\sin\phi_s$	$(4/3)(\cos\theta_1+\cos\theta_2)^2$
9	$\lvert A_S\rvert\lvert A_{SS}\rvert$	0	$\sin(\delta_S-\delta_{SS})\sin\phi_s$	$\cos(\delta_{SS}-\delta_S)$	$\sin(\delta_{SS}-\delta_S)\cos\phi_s$	$(8/3\sqrt{3})(\cos\theta_1+\cos\theta_2)$
10	$\lvert A_0\rvert\lvert A_{SS}\rvert$	$\cos\delta_{SS}$	$-\cos\delta_{SS}\cos\phi_s$	0	$\cos\delta_{SS}\sin\phi_s$	$(8/3)\cos\theta_1\cos\theta_2$
11	$\lvert A_\parallel\rvert\lvert A_{SS}\rvert$	$\cos(\delta_{2,1}-\delta_{SS})$	$-\cos(\delta_{2,1}-\delta_{SS})\cos\phi_s$	0	$\cos(\delta_{2,1}-\delta_{SS})\sin\phi_s$	$(4\sqrt{2}/3)\sin\theta_1\sin\theta_2\cos\Phi$
12	$\lvert A_\perp\rvert\lvert A_{SS}\rvert$	0	$-\cos(\delta_2-\delta_{SS})\sin\phi_s$	$\sin(\delta_2-\delta_{SS})$	$-\cos(\delta_2-\delta_{SS})\cos\phi_s$	$-(4\sqrt{2}/3)\sin\theta_1\sin\theta_2\sin\Phi$
13	$\lvert A_0\rvert\lvert A_S\rvert$	0	$-\sin\delta_S\sin\phi_s$	$\cos\delta_S$	$-\sin\delta_S\cos\phi_s$	$(8/\sqrt{3})\cos\theta_1\cos\theta_2\times(\cos\theta_1+\cos\theta_2)$
14	$\lvert A_\parallel\rvert\lvert A_S\rvert$	0	$\sin(\delta_{2,1}-\delta_S)\sin\phi_s$	$\cos(\delta_{2,1}-\delta_S)$	$\sin(\delta_{2,1}-\delta_S)\cos\phi_s$	$(4\sqrt{2}/\sqrt{3})\sin\theta_1\sin\theta_2\times(\cos\theta_1+\cos\theta_2)\cos\Phi$
15	$\lvert A_\perp\rvert\lvert A_S\rvert$	$\sin(\delta_2-\delta_S)$	$\sin(\delta_2-\delta_S)\cos\phi_s$	0	$-\sin(\delta_2-\delta_S)\sin\phi_s$	$-(4\sqrt{2}/\sqrt{3})\sin\theta_1\sin\theta_2\times(\cos\theta_1+\cos\theta_2)\sin\Phi$

$-\Delta\Gamma_s, -\delta_\parallel, \pi-\delta_\perp, -\delta_S, -\delta_{SS}$). This twofold ambiguity is resolved in the fit as Gaussian constraints are applied for the B_s^0 average decay width and decay width difference to the values measured in $B_s^0 \to J/\psi\phi$ decays, $\Gamma_s = 0.663 \pm 0.008\ \text{ps}^{-1}$ and $\Delta\Gamma_s = 0.100 \pm 0.017\ \text{ps}^{-1}$, with a correlation coefficient $\rho(\Delta\Gamma_s, \Gamma_s) = -0.39$ [6]. Similarly, the B_s^0 oscillation frequency Δm_s is constrained to the value $\Delta m_s = 17.73 \pm 0.05\ \text{ps}^{-1}$ [22].

A correction factor is multiplied to the interference terms in Table I between the P- and S-wave (and the P- and SS-wave) contributions to account for the finite m_{KK} mass window considered in the amplitude integration. This factor is calculated from the interference between the different m_{KK} line shapes of the vector and scalar contributions. The validity of the fit model has been extensively tested using simulated data samples.

The acceptance as a function of the helicity angles is not completely uniform due to the forward geometry of the detector and the momentum cuts placed to the final state particles. A three-dimensional acceptance function is determined using simulation. The acceptance factors are included in the fit as a normalization of the PDF for each of the angular terms. The acceptance function varies by less than 20% across the phase space.

The event reconstruction, trigger, and offline selections introduce a decay time dependent acceptance. In particular for short decay times, the acceptance vanishes due to the trigger, which requires tracks with significant displacement from any PV. Therefore, the decay time acceptance is determined using simulation and incorporated by multiplying the signal PDF with a binned acceptance histogram. The fractions of different triggers are found to be in agreement between data and simulation.

The parameters of a double Gaussian function used to model the decay time resolution are determined from simulation studies. A single Gaussian function with a resolution of 40 fs is found to have a similar effect on physics parameters and is applied to the data fit.

The ϕ_s measurement requires that the meson flavor be tagged as either a B_s^0 or $\bar{B}_s^0$ meson at production. To achieve this, both the opposite side (OS) and same side kaon (SSK) flavor tagging methods are used [23,24]. In OS tagging the $\bar{b}$-quark hadron produced in association with the signal b-quark is exploited through the charge of a muon or electron produced in semileptonic decays, the charge of a kaon from a subsequent charmed hadron decay, and the momentum-weighted charge of all tracks in an inclusively reconstructed decay vertex. The SSK tagging makes use of kaons formed from the s quark produced in association with the B_s^0 meson. The kaon charge identifies the flavor of the signal B_s^0 meson.

The event-by-event mistag is the probability that the decision of the tagging algorithm is incorrect and is determined by a neural network trained on simulated events and calibrated with control samples [23]. The value of the event-by-event mistag is used in the fit as an observable and the uncertainties on the calibration parameters are

TABLE II. Fit results with statistical and systematic uncertainties. A 68% statistical confidence interval is quoted for ϕ_s. Amplitudes are defined at $t = 0$.

Parameter	Value	σ_{stat}	σ_{syst}
ϕ_s [rad] (68% C.L.)		$[-2.37, -0.92]$	0.22
$\lvert A_0\rvert^2$	0.329	0.033	0.017
$\lvert A_\perp\rvert^2$	0.358	0.046	0.018
$\lvert A_S\rvert^2$	0.016	$^{+0.024}_{-0.012}$	0.009
δ_1 [rad]	2.19	0.44	0.12
δ_2 [rad]	-1.47	0.48	0.10
δ_S [rad]	0.65	$^{+0.89}_{-1.65}$	0.33

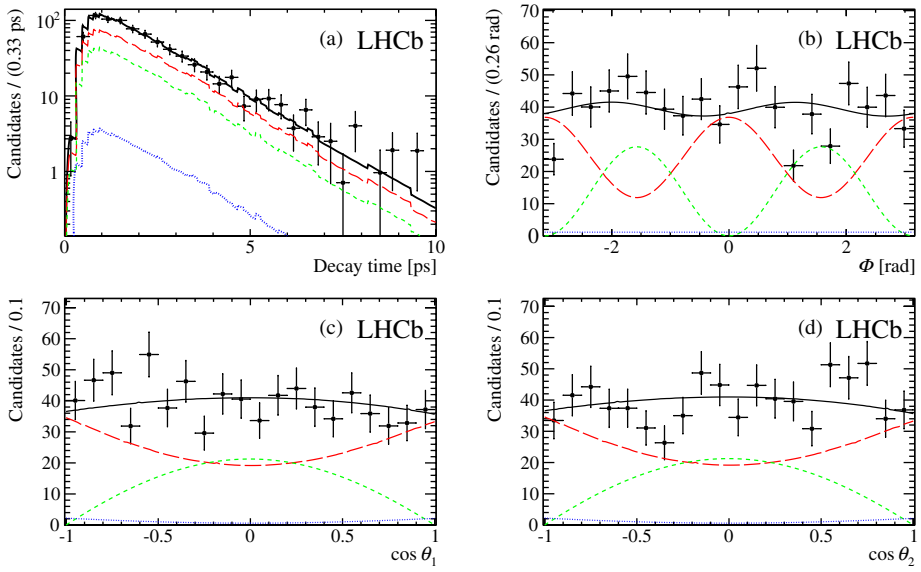

FIG. 2 (color online). One-dimensional projections of the $B_s^0 \to \phi\phi$ fit for (a) decay time, (b) helicity angle Φ, and the cosine of the helicity angles (c) θ_1 and (d) θ_2. The data are marked as points, while the solid lines represent the projections of the best fit. The CP-even P-wave, the CP-odd P-wave and S-wave components are shown by the long dashed, short dashed, and dotted lines, respectively.

propagated to the statistical uncertainties of the physics parameters, following the procedure described in Ref. [6]. For events tagged by both the OS and SSK methods, a combined tagging decision is made. The total tagging power is $\varepsilon_{\rm tag}\mathcal{D}^2 = (3.29 \pm 0.48)\%$, with a tagging efficiency of $\varepsilon_{\rm tag} = (49.7 \pm 5.0)\%$ and a dilution $\mathcal{D} = (1 - 2\omega)$ where ω is the average mistag probability. Untagged events are included in the analysis as they increase the sensitivity to ϕ_s through the b_i terms in Eq. (2).

The total S-wave fraction is determined to be $(1.6^{+2.4}_{-1.2})\%$ where the double S-wave contribution A_{SS} is set to zero, since the fit shows little sensitivity to A_{SS}. A fit to the two-dimensional mass m_{KK} for both kaon pairs where background is subtracted using sidebands is performed and yields a consistent S-wave fraction of $(2.1 \pm 1.2)\%$.

The results of the fit for the main observables are shown in Table II. Figure 2 shows the distributions for the decay time and helicity angles with the projections for the best fit PDF overlaid. The likelihood profile for the CP-violating weak phase ϕ_s, shown in Fig. 3, is not parabolic. To obtain a confidence level a correction is applied due to a small undercoverage of the likelihood profile using the method described in Ref. [25]. Including systematic uncertainties (discussed below) and assuming the values of the polarization amplitudes and strong phases observed in data, an interval of $[-2.46, -0.76]$ rad at a 68% confidence level is obtained for ϕ_s. The polarization amplitudes and phases, shown in Table II, differ from those reported in Ref. [9] as ϕ_s is not constrained to zero.

The uncertainties related to the calibration of the tagging and the assumed values of Γ_s, $\Delta\Gamma_s$, and Δm_s are absorbed into the statistical uncertainty, described above. Systematic uncertainties are determined and the sum in quadrature of all sources is reported in Table II for each observable. To check that the background is properly accounted for, an additional fit is performed where the angular and time distributions are parametrized using the B_s^0 mass sidebands. This gives results in agreement with those presented here and no further systematic uncertainty is assigned. The uncertainty due to the modeling of the S-wave component is evaluated by allowing the SS-wave component to vary in the fit. The difference between the two fits leads to the dominant uncertainty on ϕ_s of 0.20 rad. The systematic uncertainty due to the decay time acceptance is found by taking the difference in the values of fitted parameters between the nominal fit, using a binned time acceptance, and a fit in which the time acceptance is explicitly parametrized. This is found to be 0.09 rad for ϕ_s. Possible differences in the simulated decay time resolution compared to the data are studied by varying the resolution according to the discrepancies observed in the $B_s^0 \to J/\psi\phi$ analysis [6]. This leads to a systematic uncertainty of 0.01 rad for ϕ_s.

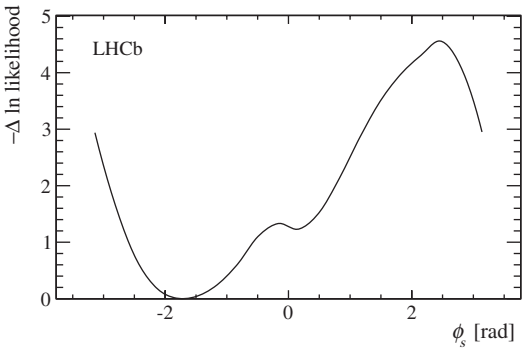

FIG. 3. Negative Δ ln likelihood scan of ϕ_s. Only the statistical uncertainty is included.

The distributions of maximum p_T and χ^2/ndf of the final state tracks and the p_T and η of the B_s^0 candidate are reweighted to better match the data. From this, the angular acceptance is recalculated, leading to small changes in the results (0.02 rad for ϕ_s), which are assigned as systematic uncertainty. Biases in the fit method are studied using simulated pseudoexperiments that lead to an uncertainty of 0.02 rad for ϕ_s. Further small systematic uncertainties (0.02 rad for ϕ_s) are due to the limited number of events in the simulation sample used for the determination of the angular acceptance and to the choice of a single versus a double Gaussian function for the mass PDF, which is used to assign the signal weights. The total systematic uncertainty on ϕ_s is 0.22 rad, significantly smaller than the statistical uncertainty.

In summary, we present the first study of CP violation in the decay time distribution of hadronic $B_s^0 \to \phi\phi$ decays. The CP-violating phase ϕ_s is restricted to the interval of $[-2.46, -0.76]$ rad at 68% C.L. The p value of the standard model prediction [8] is 16%, taking the values of the strong phases and polarization amplitudes observed in data and assuming that systematic uncertainties are negligible. The precision of the ϕ_s measurement is dominated by the statistical uncertainty and is expected to improve with larger LHCb data sets.

We express our gratitude to our colleagues in the CERN accelerator departments for the excellent performance of the LHC. We thank the technical and administrative staff at the LHCb institutes. We acknowledge support from CERN and from the national agencies CAPES, CNPq, FAPERJ, and FINEP (Brazil); NSFC (China); CNRS/IN2P3 and Region Auvergne (France); BMBF, DFG, HGF, and MPG (Germany); SFI (Ireland); INFN (Italy); FOM and NWO (The Netherlands); SCSR (Poland); ANCS/IFA (Romania); MinES, Rosatom, RFBR, and NRC "Kurchatov Institute" (Russia); MinECo, XuntaGal, and GENCAT (Spain); SNSF and SER (Switzerland); NAS Ukraine (Ukraine); STFC (United Kingdom); NSF (USA). We also acknowledge the support received from the ERC under FP7. The Tier1 Computing Centres are supported by IN2P3 (France), KIT and BMBF (Germany), INFN (Italy), NWO and SURF (The Netherlands), PIC (Spain), GridPP (United Kingdom). We are thankful for the computing resources put at our disposal by Yandex LLC (Russia), as well as to the communities behind the multiple open source software packages that we depend on.

[1] M. Bartsch, G. Buchalla, and C. Kraus, arXiv:0810.0249.
[2] M. Beneke, J. Rohrer, and D. Yang, Nucl. Phys. **B774**, 64 (2007).
[3] H.-Y. Cheng and C.-K. Chua, Phys. Rev. D **80**, 114026 (2009).
[4] M. Kobayashi and T. Maskawa, Prog. Theor. Phys. **49**, 652 (1973); N. Cabibbo, Phys. Rev. Lett. **10**, 531 (1963).
[5] J. Charles *et al.*, Phys. Rev. D **84**, 033005 (2011).
[6] R. Aaij *et al.* (LHCb Collaboration), Report No. LHCb-PAPER-2013-002 (to be published).
[7] R. Aaij *et al.* (LHCb Collaboration), Eur. Phys. J. C **73**, 2373 (2013).
[8] M. Raidal, Phys. Rev. Lett. **89**, 231803 (2002).
[9] R. Aaij *et al.* (LHCb Collaboration), Phys. Lett. B **713**, 369 (2012).
[10] A. A. Alves, Jr. *et al.* (LHCb Collaboration), J. Instrum. **3**, S08005 (2008).
[11] R. Aaij *et al.*, J. Instrum. **8**, P04022 (2013).
[12] T. Sjöstrand, S. Mrenna, and P. Skands, J. High Energy Phys. 05 (2006) 026.
[13] I. Belyaev *et al.*, in *Proceedings of the 2010 IEEE Nuclear Science Symposium Conference* (IEEE, New York, 2010), p. 1155.
[14] D. J. Lange, Nucl. Instrum. Methods Phys. Res., Sect. A **462**, 152 (2001).
[15] J. Allison *et al.* (GEANT4 Collaboration), IEEE Trans. Nucl. Sci. **53**, 270 (2006); S. Agostinelli *et al.* (GEANT4 collaboration), Nucl. Instrum. Methods Phys. Res., Sect. A **506**, 250 (2003).
[16] M. Clemencic, G. Corti, S. Easo, C. R. Jones, S. Miglioranzi, M. Pappagallo, and P. Robbe, J. Phys. Conf. Ser. **331**, 032023 (2011).
[17] M. Adinolfi *et al.*, Eur. Phys. J. C **73**, 2431 (2013).
[18] L. Breiman, J. H. Friedman, R. A. Olshen, and C. J. Stone, *Classification and Regression Trees* (Wadsworth International Group, Belmont, CA, 1984).
[19] M. Pivk and F. R. Le Diberder, Nucl. Instrum. Methods Phys. Res., Sect. A **555**, 356 (2005).
[20] Y. Xie, arXiv:0905.0724.
[21] C.-W. Chiang and L. Wolfenstein, Phys. Rev. D **61**, 074031 (2000).
[22] LHCb Collaboration, Report No. LHCb-CONF-2011-050.
[23] R. Aaij *et al.* (LHCb Collaboration), Eur. Phys. J. C **72**, 2022 (2012).
[24] LHCb Collaboration, Report No. LHCb-CONF-2012-033.
[25] G. J. Feldman and R. D. Cousins, Phys. Rev. D **57**, 3873 (1998).

R. Aaij,[40] C. Abellan Beteta,[35,n] B. Adeva,[36] M. Adinolfi,[45] C. Adrover,[6] A. Affolder,[51] Z. Ajaltouni,[5] J. Albrecht,[9] F. Alessio,[37] M. Alexander,[50] S. Ali,[40] G. Alkhazov,[29] P. Alvarez Cartelle,[36] A. A. Alves, Jr.,[24,37] S. Amato,[2] S. Amerio,[21] Y. Amhis,[7] L. Anderlini,[17,f] J. Anderson,[39] R. Andreassen,[59] R. B. Appleby,[53] O. Aquines Gutierrez,[10] F. Archilli,[18] A. Artamonov,[34] M. Artuso,[56] E. Aslanides,[6] G. Auriemma,[24,m] S. Bachmann,[11] J. J. Back,[47] C. Baesso,[57] V. Balagura,[30] W. Baldini,[16] R. J. Barlow,[53] C. Barschel,[37] S. Barsuk,[7] W. Barter,[46] Th. Bauer,[40] A. Bay,[38] J. Beddow,[50] F. Bedeschi,[22] I. Bediaga,[1] S. Belogurov,[30] K. Belous,[34] I. Belyaev,[30] E. Ben-Haim,[8] M. Benayoun,[8] G. Bencivenni,[18] S. Benson,[49] J. Benton,[45] A. Berezhnoy,[31] R. Bernet,[39] M.-O. Bettler,[46]

M. van Beuzekom,[40] A. Bien,[11] S. Bifani,[12] T. Bird,[53] A. Bizzeti,[17,h] P. M. Bjørnstad,[53] T. Blake,[37] F. Blanc,[38] J. Blouw,[11] S. Blusk,[56] V. Bocci,[24] A. Bondar,[33] N. Bondar,[29] W. Bonivento,[15] S. Borghi,[53] A. Borgia,[56] T. J. V. Bowcock,[51] E. Bowen,[39] C. Bozzi,[16] T. Brambach,[9] J. van den Brand,[41] J. Bressieux,[38] D. Brett,[53] M. Britsch,[10] T. Britton,[56] N. H. Brook,[45] H. Brown,[51] I. Burducea,[28] A. Bursche,[39] G. Busetto,[21,q] J. Buytaert,[37] S. Cadeddu,[15] O. Callot,[7] M. Calvi,[20,j] M. Calvo Gomez,[35,n] A. Camboni,[35] P. Campana,[18,37] D. Campora Perez,[37] A. Carbone,[14,c] G. Carboni,[23,k] R. Cardinale,[19,i] A. Cardini,[15] H. Carranza-Mejia,[49] L. Carson,[52] K. Carvalho Akiba,[2] G. Casse,[51] M. Cattaneo,[37] Ch. Cauet,[9] M. Charles,[54] Ph. Charpentier,[37] P. Chen,[3,38] N. Chiapolini,[39] M. Chrzaszcz,[25] K. Ciba,[37] X. Cid Vidal,[37] G. Ciezarek,[52] P. E. L. Clarke,[49] M. Clemencic,[37] H. V. Cliff,[46] J. Closier,[37] C. Coca,[28] V. Coco,[40] J. Cogan,[6] E. Cogneras,[5] P. Collins,[37] A. Comerma-Montells,[35] A. Contu,[15] A. Cook,[45] M. Coombes,[45] S. Coquereau,[8] G. Corti,[37] B. Couturier,[37] G. A. Cowan,[49] D. Craik,[47] S. Cunliffe,[52] R. Currie,[49] C. D'Ambrosio,[37] P. David,[8] P. N. Y. David,[40] A. Davis,[59] I. De Bonis,[4] K. De Bruyn,[40] S. De Capua,[53] M. De Cian,[39] J. M. De Miranda,[1] L. De Paula,[2] W. De Silva,[59] P. De Simone,[18] D. Decamp,[4] M. Deckenhoff,[9] L. Del Buono,[8] D. Derkach,[14] O. Deschamps,[5] F. Dettori,[41] A. Di Canto,[11] H. Dijkstra,[37] M. Dogaru,[28] S. Donleavy,[51] F. Dordei,[11] A. Dosil Suárez,[36] D. Dossett,[47] A. Dovbnya,[42] F. Dupertuis,[38] R. Dzhelyadin,[34] A. Dziurda,[25] A. Dzyuba,[29] S. Easo,[48,37] U. Egede,[52] V. Egorychev,[30] S. Eidelman,[33] D. van Eijk,[40] S. Eisenhardt,[49] U. Eitschberger,[9] R. Ekelhof,[9] L. Eklund,[50,37] I. El Rifai,[5] Ch. Elsasser,[39] D. Elsby,[44] A. Falabella,[14,e] C. Färber,[11] G. Fardell,[49] C. Farinelli,[40] S. Farry,[12] V. Fave,[38] D. Ferguson,[49] V. Fernandez Albor,[36] F. Ferreira Rodrigues,[1] M. Ferro-Luzzi,[37] S. Filippov,[32] C. Fitzpatrick,[37] M. Fontana,[10] F. Fontanelli,[19,i] R. Forty,[37] O. Francisco,[2] M. Frank,[37] C. Frei,[37] M. Frosini,[17,f] S. Furcas,[20] E. Furfaro,[23] A. Gallas Torreira,[36] D. Galli,[14,c] M. Gandelman,[2] P. Gandini,[56] Y. Gao,[3] J. Garofoli,[56] P. Garosi,[53] J. Garra Tico,[46] L. Garrido,[35] C. Gaspar,[37] R. Gauld,[54] E. Gersabeck,[11] M. Gersabeck,[53] T. Gershon,[47,37] Ph. Ghez,[4] V. Gibson,[46] V. V. Gligorov,[37] C. Göbel,[57] D. Golubkov,[30] A. Golutvin,[52,30,37] A. Gomes,[2] H. Gordon,[54] M. Grabalosa Gándara,[5] R. Graciani Diaz,[35] L. A. Granado Cardoso,[37] E. Graugés,[35] G. Graziani,[17] A. Grecu,[28] E. Greening,[54] S. Gregson,[46] O. Grünberg,[58] B. Gui,[56] E. Gushchin,[32] Yu. Guz,[34,37] T. Gys,[37] C. Hadjivasiliou,[56] G. Haefeli,[38] C. Haen,[37] S. C. Haines,[46] S. Hall,[52] T. Hampson,[45] S. Hansmann-Menzemer,[11] N. Harnew,[54] S. T. Harnew,[45] J. Harrison,[53] T. Hartmann,[58] J. He,[37] V. Heijne,[40] K. Hennessy,[51] P. Henrard,[5] J. A. Hernando Morata,[36] E. van Herwijnen,[37] E. Hicks,[51] D. Hill,[54] M. Hoballah,[5] C. Hombach,[53] P. Hopchev,[4] W. Hulsbergen,[40] P. Hunt,[54] T. Huse,[51] N. Hussain,[54] D. Hutchcroft,[51] D. Hynds,[50] V. Iakovenko,[43] M. Idzik,[26] P. Ilten,[12] R. Jacobsson,[37] A. Jaeger,[11] E. Jans,[40] P. Jaton,[38] F. Jing,[3] M. John,[54] D. Johnson,[54] C. R. Jones,[46] B. Jost,[37] M. Kaballo,[9] S. Kandybei,[42] M. Karacson,[37] T. M. Karbach,[37] I. R. Kenyon,[44] U. Kerzel,[37] T. Ketel,[41] A. Keune,[38] B. Khanji,[20] O. Kochebina,[7] I. Komarov,[38] R. F. Koopman,[41] P. Koppenburg,[40] M. Korolev,[31] A. Kozlinskiy,[40] L. Kravchuk,[32] K. Kreplin,[11] M. Kreps,[47] G. Krocker,[11] P. Krokovny,[33] F. Kruse,[9] M. Kucharczyk,[20,25,j] V. Kudryavtsev,[33] T. Kvaratskheliya,[30,37] V. N. La Thi,[38] D. Lacarrere,[37] G. Lafferty,[53] A. Lai,[15] D. Lambert,[49] R. W. Lambert,[41] E. Lanciotti,[37] G. Lanfranchi,[18,37] C. Langenbruch,[37] T. Latham,[47] C. Lazzeroni,[44] R. Le Gac,[6] J. van Leerdam,[40] J.-P. Lees,[4] R. Lefèvre,[5] A. Leflat,[31] J. Lefrançois,[7] S. Leo,[22] O. Leroy,[6] B. Leverington,[11] Y. Li,[3] L. Li Gioi,[5] M. Liles,[51] R. Lindner,[37] C. Linn,[11] B. Liu,[3] G. Liu,[37] S. Lohn,[37] I. Longstaff,[50] J. H. Lopes,[2] E. Lopez Asamar,[35] N. Lopez-March,[38] H. Lu,[3] D. Lucchesi,[21,q] J. Luisier,[38] H. Luo,[49] F. Machefert,[7] I. V. Machikhiliyan,[4,30] F. Maciuc,[28] O. Maev,[29,37] S. Malde,[54] G. Manca,[15,d] G. Mancinelli,[6] U. Marconi,[14] R. Märki,[38] J. Marks,[11] G. Martellotti,[24] A. Martens,[8] L. Martin,[54] A. Martín Sánchez,[7] M. Martinelli,[40] D. Martinez Santos,[41] D. Martins Tostes,[2] A. Massafferri,[1] R. Matev,[37] Z. Mathe,[37] C. Matteuzzi,[20] E. Maurice,[6] A. Mazurov,[16,32,37,e] J. McCarthy,[44] R. McNulty,[12] A. Mcnab,[53] B. Meadows,[59,54] F. Meier,[9] M. Meissner,[11] M. Merk,[40] D. A. Milanes,[8] M.-N. Minard,[4] J. Molina Rodriguez,[57] S. Monteil,[5] D. Moran,[53] P. Morawski,[25] M. J. Morello,[22,s] R. Mountain,[56] I. Mous,[40] F. Muheim,[49] K. Müller,[39] R. Muresan,[28] B. Muryn,[26] B. Muster,[38] P. Naik,[45] T. Nakada,[38] R. Nandakumar,[48] I. Nasteva,[1] M. Needham,[49] N. Neufeld,[37] A. D. Nguyen,[38] T. D. Nguyen,[38] C. Nguyen-Mau,[38,p] M. Nicol,[7] V. Niess,[5] R. Niet,[9] N. Nikitin,[31] T. Nikodem,[11] A. Nomerotski,[54] A. Novoselov,[34] A. Oblakowska-Mucha,[26] V. Obraztsov,[34] S. Oggero,[40] S. Ogilvy,[50] O. Okhrimenko,[43] R. Oldeman,[15,d] M. Orlandea,[28] J. M. Otalora Goicochea,[2] P. Owen,[52] A. Oyanguren,[35,o] B. K. Pal,[56] A. Palano,[13,b] M. Palutan,[18] J. Panman,[37] A. Papanestis,[48] M. Pappagallo,[50] C. Parkes,[53] C. J. Parkinson,[52] G. Passaleva,[17] G. D. Patel,[51] M. Patel,[52] G. N. Patrick,[48] C. Patrignani,[19,i] C. Pavel-Nicorescu,[28] A. Pazos Alvarez,[36] A. Pellegrino,[40] G. Penso,[24,l] M. Pepe Altarelli,[37] S. Perazzini,[14,c] D. L. Perego,[20,j] E. Perez Trigo,[36] A. Pérez-Calero Yzquierdo,[35] P. Perret,[5] M. Perrin-Terrin,[6] G. Pessina,[20] K. Petridis,[52] A. Petrolini,[19,i] A. Phan,[56] E. Picatoste Olloqui,[35] B. Pietrzyk,[4] T. Pilař,[47] D. Pinci,[24] S. Playfer,[49] M. Plo Casasus,[36]

F. Polci,[8] G. Polok,[25] A. Poluektov,[47,33] E. Polycarpo,[2] D. Popov,[10] B. Popovici,[28] C. Potterat,[35] A. Powell,[54] J. Prisciandaro,[38] V. Pugatch,[43] A. Puig Navarro,[38] G. Punzi,[22,r] W. Qian,[4] J. H. Rademacker,[45] B. Rakotomiaramanana,[38] M. S. Rangel,[2] I. Raniuk,[42] N. Rauschmayr,[37] G. Raven,[41] S. Redford,[54] M. M. Reid,[47] A. C. dos Reis,[1] S. Ricciardi,[48] A. Richards,[52] K. Rinnert,[51] V. Rives Molina,[35] D. A. Roa Romero,[5] P. Robbe,[7] E. Rodrigues,[53] P. Rodriguez Perez,[36] S. Roiser,[37] V. Romanovsky,[34] A. Romero Vidal,[36] J. Rouvinet,[38] T. Ruf,[37] F. Ruffini,[22] H. Ruiz,[35] P. Ruiz Valls,[35,o] G. Sabatino,[24,k] J. J. Saborido Silva,[36] N. Sagidova,[29] P. Sail,[50] B. Saitta,[15,d] C. Salzmann,[39] B. Sanmartin Sedes,[36] M. Sannino,[19,i] R. Santacesaria,[24] C. Santamarina Rios,[36] E. Santovetti,[23,k] M. Sapunov,[6] A. Sarti,[18,l] C. Satriano,[24,m] A. Satta,[23] M. Savrie,[16,e] D. Savrina,[30,31] P. Schaack,[52] M. Schiller,[41] H. Schindler,[37] M. Schlupp,[9] M. Schmelling,[10] B. Schmidt,[37] O. Schneider,[38] A. Schopper,[37] M.-H. Schune,[7] R. Schwemmer,[37] B. Sciascia,[18] A. Sciubba,[24] M. Seco,[36] A. Semennikov,[30] K. Senderowska,[26] I. Sepp,[52] N. Serra,[39] J. Serrano,[6] P. Seyfert,[11] M. Shapkin,[34] I. Shapoval,[42] P. Shatalov,[30] Y. Shcheglov,[29] T. Shears,[51,37] L. Shekhtman,[33] O. Shevchenko,[42] V. Shevchenko,[30] A. Shires,[52] R. Silva Coutinho,[47] T. Skwarnicki,[56] N. A. Smith,[51] E. Smith,[54,48] M. Smith,[53] M. D. Sokoloff,[59] F. J. P. Soler,[50] F. Soomro,[18] D. Souza,[45] B. Souza De Paula,[2] B. Spaan,[9] A. Sparkes,[49] P. Spradlin,[50] F. Stagni,[37] S. Stahl,[11] O. Steinkamp,[39] S. Stoica,[28] S. Stone,[56] B. Storaci,[39] M. Straticiuc,[28] U. Straumann,[39] V. K. Subbiah,[37] S. Swientek,[9] V. Syropoulos,[41] M. Szczekowski,[27] P. Szczypka,[38,37] T. Szumlak,[26] S. T'Jampens,[4] M. Teklishyn,[7] E. Teodorescu,[28] F. Teubert,[37] C. Thomas,[54] E. Thomas,[37] J. van Tilburg,[11] V. Tisserand,[4] M. Tobin,[39] S. Tolk,[41] D. Tonelli,[37] S. Topp-Joergensen,[54] N. Torr,[54] E. Tournefier,[4,52] S. Tourneur,[38] M. T. Tran,[38] M. Tresch,[39] A. Tsaregorodtsev,[6] P. Tsopelas,[40] N. Tuning,[40] M. Ubeda Garcia,[37] A. Ukleja,[27] D. Urner,[53] U. Uwer,[11] V. Vagnoni,[14] G. Valenti,[14] R. Vazquez Gomez,[35] P. Vazquez Regueiro,[36] S. Vecchi,[16] J. J. Velthuis,[45] M. Veltri,[17,g] G. Veneziano,[38] M. Vesterinen,[37] B. Viaud,[7] D. Vieira,[2] X. Vilasis-Cardona,[35,n] A. Vollhardt,[39] D. Volyanskyy,[10] D. Voong,[45] A. Vorobyev,[29] V. Vorobyev,[33] C. Voß,[58] H. Voss,[10] R. Waldi,[58] R. Wallace,[12] S. Wandernoth,[11] J. Wang,[56] D. R. Ward,[46] N. K. Watson,[44] A. D. Webber,[53] D. Websdale,[52] M. Whitehead,[47] J. Wicht,[37] J. Wiechczynski,[25] D. Wiedner,[11] L. Wiggers,[40] G. Wilkinson,[54] M. P. Williams,[47,48] M. Williams,[55] F. F. Wilson,[48] J. Wishahi,[9] M. Witek,[25] S. A. Wotton,[46] S. Wright,[46] S. Wu,[3] K. Wyllie,[37] Y. Xie,[49,37] F. Xing,[54] Z. Xing,[56] Z. Yang,[3] R. Young,[49] X. Yuan,[3] O. Yushchenko,[34] M. Zangoli,[14] M. Zavertyaev,[10,a] F. Zhang,[3] L. Zhang,[56] W. C. Zhang,[12] Y. Zhang,[3] A. Zhelezov,[11] A. Zhokhov,[30] L. Zhong,[3] and A. Zvyagin[37]

(LHCb Collaboration)

[1]*Centro Brasileiro de Pesquisas Físicas (CBPF), Rio de Janeiro, Brazil*
[2]*Universidade Federal do Rio de Janeiro (UFRJ), Rio de Janeiro, Brazil*
[3]*Center for High Energy Physics, Tsinghua University, Beijing, China*
[4]*LAPP, Université de Savoie, CNRS/IN2P3, Annecy-Le-Vieux, France*
[5]*Clermont Université, Université Blaise Pascal, CNRS/IN2P3, LPC, Clermont-Ferrand, France*
[6]*CPPM, Aix-Marseille Université, CNRS/IN2P3, Marseille, France*
[7]*LAL, Université Paris-Sud, CNRS/IN2P3, Orsay, France*
[8]*LPNHE, Université Pierre et Marie Curie, Université Paris Diderot, CNRS/IN2P3, Paris, France*
[9]*Fakultät Physik, Technische Universität Dortmund, Dortmund, Germany*
[10]*Max-Planck-Institut für Kernphysik (MPIK), Heidelberg, Germany*
[11]*Physikalisches Institut, Ruprecht-Karls-Universität Heidelberg, Heidelberg, Germany*
[12]*School of Physics, University College Dublin, Dublin, Ireland*
[13]*Sezione INFN di Bari, Bari, Italy*
[14]*Sezione INFN di Bologna, Bologna, Italy*
[15]*Sezione INFN di Cagliari, Cagliari, Italy*
[16]*Sezione INFN di Ferrara, Ferrara, Italy*
[17]*Sezione INFN di Firenze, Firenze, Italy*
[18]*Laboratori Nazionali dell'INFN di Frascati, Frascati, Italy*
[19]*Sezione INFN di Genova, Genova, Italy*
[20]*Sezione INFN di Milano Bicocca, Milano, Italy*
[21]*Sezione INFN di Padova, Padova, Italy*
[22]*Sezione INFN di Pisa, Pisa, Italy*
[23]*Sezione INFN di Roma Tor Vergata, Roma, Italy*
[24]*Sezione INFN di Roma La Sapienza, Roma, Italy*
[25]*Henryk Niewodniczanski Institute of Nuclear Physics Polish Academy of Sciences, Kraków, Poland*
[26]*AGH University of Science and Technology, Kraków, Poland*

[27]National Center for Nuclear Research (NCBJ), Warsaw, Poland
[28]Horia Hulubei National Institute of Physics and Nuclear Engineering, Bucharest-Magurele, Romania
[29]Petersburg Nuclear Physics Institute (PNPI), Gatchina, Russia
[30]Institute of Theoretical and Experimental Physics (ITEP), Moscow, Russia
[31]Institute of Nuclear Physics, Moscow State University (SINP MSU), Moscow, Russia
[32]Institute for Nuclear Research of the Russian Academy of Sciences (INR RAN), Moscow, Russia
[33]Budker Institute of Nuclear Physics (SB RAS) and Novosibirsk State University, Novosibirsk, Russia
[34]Institute for High Energy Physics (IHEP), Protvino, Russia
[35]Universitat de Barcelona, Barcelona, Spain
[36]Universidad de Santiago de Compostela, Santiago de Compostela, Spain
[37]European Organization for Nuclear Research (CERN), Geneva, Switzerland
[38]Ecole Polytechnique Fédérale de Lausanne (EPFL), Lausanne, Switzerland
[39]Physik-Institut, Universität Zürich, Zürich, Switzerland
[40]Nikhef National Institute for Subatomic Physics, Amsterdam, The Netherlands
[41]Nikhef National Institute for Subatomic Physics and VU University Amsterdam, Amsterdam, The Netherlands
[42]NSC Kharkiv Institute of Physics and Technology (NSC KIPT), Kharkiv, Ukraine
[43]Institute for Nuclear Research of the National Academy of Sciences (KINR), Kyiv, Ukraine
[44]University of Birmingham, Birmingham, United Kingdom
[45]H. H. Wills Physics Laboratory, University of Bristol, Bristol, United Kingdom
[46]Cavendish Laboratory, University of Cambridge, Cambridge, United Kingdom
[47]Department of Physics, University of Warwick, Coventry, United Kingdom
[48]STFC Rutherford Appleton Laboratory, Didcot, United Kingdom
[49]School of Physics and Astronomy, University of Edinburgh, Edinburgh, United Kingdom
[50]School of Physics and Astronomy, University of Glasgow, Glasgow, United Kingdom
[51]Oliver Lodge Laboratory, University of Liverpool, Liverpool, United Kingdom
[52]Imperial College London, London, United Kingdom
[53]School of Physics and Astronomy, University of Manchester, Manchester, United Kingdom
[54]Department of Physics, University of Oxford, Oxford, United Kingdom
[55]Massachusetts Institute of Technology, Cambridge, Massachusetts, USA
[56]Syracuse University, Syracuse, New York, USA
[57]Pontifícia Universidade Católica do Rio de Janeiro (PUC-Rio), Rio de Janeiro, Brazil, associated to Universidade Federal do Rio de Janeiro (UFRJ), Rio de Janeiro, Brazil
[58]Institut für Physik, Universität Rostock, Rostock, Germany, associated to Physikalisches Institut, Ruprecht-Karls-Universität Heidelberg, Heidelberg, Germany
[59]University of Cincinnati, Cincinnati, Ohio, USA, associated to Syracuse University, Syracuse, New York, USA

[a]P. N. Lebedev Physical Institute, Russian Academy of Science (LPI RAS), Moscow, Russia.
[b]Università di Bari, Bari, Italy.
[c]Università di Bologna, Bologna, Italy.
[d]Università di Cagliari, Cagliari, Italy.
[e]Università di Ferrara, Ferrara, Italy.
[f]Università di Firenze, Firenze, Italy.
[g]Università di Urbino, Urbino, Italy.
[h]Università di Modena e Reggio Emilia, Modena, Italy.
[i]Università di Genova, Genova, Italy.
[j]Università di Milano Bicocca, Milano, Italy.
[k]Università di Roma Tor Vergata, Roma, Italy.
[l]Università di Roma La Sapienza, Roma, Italy.
[m]Università della Basilicata, Potenza, Italy.
[n]LIFAELS, La Salle, Universitat Ramon Llull, Barcelona, Spain.
[o]IFIC, Universitat de Valencia-CSIC, Valencia, Spain.
[p]Hanoi University of Science, Hanoi, Vietnam.
[q]Università di Padova, Padova, Italy.
[r]Università di Pisa, Pisa, Italy.
[s]Scuola Normale Superiore, Pisa, Italy.